Mon. Not. R. Astron. Soc. **000**, 000–000 (1994) Printed 21 August 2001 (MN plain TEX macros v1.6)

Series solutions for polytropes and the isothermal sphere.

C. Hunter
Department of Mathematics, Florida State University, Tallahassee, FL 32306-4510, USA

ABSTRACT

The Lane–Emden equation for polytropic index $n > 1$ and its $n \to \infty$ limit of the isothermal sphere equation are singular at some *negative* value of the radius squared. This singularity prevents the real power series solutions about the centre from converging all the way to the outer surface when $n > 1.9121$. However, a simple Euler transformation gives series that do converge all the way to the outer radius. These Euler–transformed series converge significantly faster than the series in the contained mass derived by Roxburgh & Stockman (1999), which are limited to finite radii whenever $n > 5$ by a complex conjugate pair of singularities. We construct some compact analytical approximations to the isothermal sphere, and give one for which the density profile is accurate to 0.001 percent out to the limit of stability against gravothermal collapse.

Key words: methods: analytical - stars: interiors.

1 INTRODUCTION

Polytropes and isothermal spheres provide simple models for stars (Kippenhahn & Weigert 1990) and for spherical galaxies (Binney & Tremaine 1987), though modern texts no longer give them the same thorough treatment that the classical works of Emden (1907) and Chandrasekhar (1939) do. Closed form analytical solutions are known for only three special cases of the index n, of which $n = 5$ is the only one for which the Lane–Emden equation is nonlinear. Otherwise that equation must be solved either by series expansion or numerically. Because the centre is a singular point of the Lane–Emden equation, a series solution is needed to start a numerical solution from there. If this series converges throughout the star, nothing more is needed. Long ago See (1905) computed a 26–term series for the $n = 1.5$ polytrope and found that it can be used all the way to its zero density surface. With accurate computation, this truncated series indeed gives seven decimal digit accuracy over the inner 90% of this polytrope and six decimal digit accuracy to its surface.

Roxburgh & Stockman (1999, hereafter RS) computed large numbers of series coefficients for many other n values, but found that the series cease to converge before the surface of the star is reached when $2 \le n \le 5$. In Section 2 we explain this lack of convergence. It is due to a singularity of the form $(1 + \xi^2/x_n^2)^{-2/(n-1)}$ at the pure imaginary values $\xi = \pm i x_n$ of the scaled radius ξ. This singularity is present for all $n > 1$. It is further from the centre of the star than its surface for $n < 1.9121$, but closer for $n > 1.9121$ and the series then converges only for $\xi < x_n$. This singularity causes the regular alternation in sign of the series coefficients which RS found for $n \ge 2$. It also causes the initial alternation in sign for $n < 1.9121$ which persists until the closer, but weaker, singularity at the surface of the star eventually dominates.

In Section 3.1, we show how to use a simple bilinear Euler transformation to yield a series solution of the Lane–Emden equation which converges out to the surface of the star for polytropes of all n. We also construct an Euler–transformed series which, once its singular component has been subtracted off, converges throughout the isothermal sphere.

RS proposed expansion in powers of $m = q^{2/3}$, where $q(\xi)$ is the mass interior to the radius ξ, as a method of generating series which converge over a wider range. Their m–series appeared to converge all the way to the surface of the polytrope for all $n \le 5$. Our analysis in Appendix B confirms that this is so, but we show that their rates of convergence are considerably less than those of the Euler–transformed series for $2 < n < 5$. The m–series is an Euler–transformed series for the special $n = 5$ case of the Plummer sphere, but a marked change occurs when n exceeds 5. The m–series then develop complex singularities at finite m, and do not converge out to the surface which is now at $m = \infty$.

Our analysis of singularities of solutions yields the essential information about their analytic structure. In Section 4 we discuss the use of that information for constructing compact analytical approximations. In particular, we extend Natarajan & Lynden-Bell's (1997) simple model of the isothermal sphere to high acccuracy.

Section 5 gives our conclusions. Appendix A proves that the solution of the Lane–Emden equation is singular at some finite imaginary radius for all $n > 1$. Appendix B analyses the m–series, and when and why they converge, and at what rate. Appendix C discusses how the isothermal sphere equa-

tion arises as the $n \to \infty$ limit of the Lane–Emden equation, and its relevance to this study. Although the occurrence of this limit is widely believed, I have been unable to locate any prior discussion of it.

2 POLYTROPES AND ISOTHERMAL SPHERES

2.1 Basic equations and series solutions

The basic equation of this study is the Lane–Emden equation (Chandrasekhar 1939, Kippenhahn & Weigert 1990)

$$\frac{\mathrm{d}^2\theta}{\mathrm{d}\xi^2} + \frac{2}{\xi}\frac{\mathrm{d}\theta}{\mathrm{d}\xi} = -\theta^n. \tag{1}$$

Here θ is the negative of the scaled potential and ξ is a scaled radius. The Lane–Emden equation is essentially Poisson's equation for the gravitational potential, and θ^n is the scaled density which causes that potential. The physically relevant solution is that for which $\theta = 1$ and $d\theta/d\xi = 0$ at $\xi = 0$. This solution is analytic at $\xi = 0$, and has a Taylor series expansion

$$\theta = \sum_{k=0}^{\infty} a_k \xi^{2k}, \quad \theta^n = \sum_{k=0}^{\infty} b_k \xi^{2k}, \quad a_0 = b_0 = 1. \tag{2}$$

This Taylor series contains only even powers of ξ, and hence it is simpler to work with the independent variable $\zeta = \xi^2$. Changing to ζ as the independent variable, the Lane–Emden equation becomes

$$4\zeta\frac{\mathrm{d}^2\theta}{\mathrm{d}\zeta^2} + 6\frac{\mathrm{d}\theta}{\mathrm{d}\zeta} = -\theta^n, \quad \theta(0) = 1, \tag{3}$$

and its series solution

$$\theta(\zeta) = \sum_{k=0}^{\infty} a_k \zeta^k, \quad \theta^n = \sum_{k=0}^{\infty} b_k \zeta^k. \tag{4}$$

Many texts give explicit expressions for the first few coefficients a_k and b_k, and RS give the recursive relations for determining them all.

The standard form of the equation for the isothermal sphere (Chandrasekhar 1939, Kippenhahn & Weigert 1990) is

$$\frac{\mathrm{d}^2\tilde{\theta}}{\mathrm{d}\tilde{\xi}^2} + \frac{2}{\tilde{\xi}}\frac{\mathrm{d}\tilde{\theta}}{\mathrm{d}\tilde{\xi}} = e^{-\tilde{\theta}}, \quad \tilde{\theta}(0) = 0. \tag{5}$$

Its scaled potential $\tilde{\theta}$, which is conventionally taken to be zero at the centre, is a *positive* multiple of the gravitational potential and increases with the scaled radius $\tilde{\xi}$. The scaled density is now $e^{-\tilde{\theta}}$. We use tildes to distinguish the isothermal case because of these basic differences of definition and scaling. We discuss in Appendix C how to obtain the isothermal sphere as the $n \to \infty$ limit of a polytrope.

With $\tilde{\zeta} = \tilde{\xi}^2$ as independent variable, the isothermal sphere equation becomes

$$4\tilde{\zeta}\frac{\mathrm{d}^2\tilde{\theta}}{\mathrm{d}\tilde{\zeta}^2} + 6\frac{\mathrm{d}\tilde{\theta}}{\mathrm{d}\tilde{\zeta}} = e^{-\tilde{\theta}}. \quad \tilde{\theta}(0) = 0. \tag{6}$$

Its series solution is

$$\tilde{\theta}(\tilde{\zeta}) = \sum_{k=1}^{\infty} \tilde{a}_k \tilde{\zeta}^k, \quad e^{-\tilde{\theta}} = \sum_{k=0}^{\infty} \tilde{b}_k \tilde{\zeta}^k, \quad \tilde{b}_0 = 1, \tag{7}$$

and their coefficients are obtained by solving the following equations recursively for $k \geq 1$:

$$\tilde{a}_k = \frac{\tilde{b}_{k-1}}{2k(2k+1)}, \quad \tilde{b}_k = -\frac{1}{k}\sum_{j=0}^{k-1}(k-j)\tilde{b}_j\tilde{a}_{k-j}. \tag{8}$$

2.2 Singularities

The radius of convergence of the series (4) is the distance from $\zeta = 0$ to the closest singularity of $\theta(\zeta)$ in the complex ζ–plane. Nonlinear ordinary differential equations, such as the Lane–Emden equation for $n > 1$, can have two kinds of singularities, fixed and movable (Ablowitz & Fokas 1997). Fixed singularities of the Lane–Emden equation occur at $\zeta = 0$ and $\zeta = \infty$, due to the coefficient 4ζ of the second derivative in equation (3). The series (4) defines a function which is analytic at $\zeta = 0$, and so the only possible finite singularities of $\theta(\zeta)$ are movable ones.

Movable singularities have locations that vary from solution to solution depending on the boundary conditions. The Lane–Emden equation allows just two kinds of movable singularities. One occurs at points at which $\theta = 0$. The density, and hence θ vanishes at the surface of the star at radius $\sqrt{\zeta_s}$ say. Here θ has some non-zero slope $S = \mathrm{d}\theta/\mathrm{d}\zeta|_{\zeta=\zeta_s}$. This causes a mild singularity at $\zeta = \zeta_s$, whenever n is not an integer, because the θ^n term in (3) then gives rise to a component $-(-S)^n(\zeta_s - \zeta)^{n+2}/4\zeta_s(n+1)(n+2)$ in the expansion of the solution about $\zeta = \zeta_s$, and other non-integer powers occur at higher order.

The other kind of movable singularities are at points at which θ becomes infinite. Their nature can be deduced from the dominant balance (Hinch 1991) between the most singular terms in (3). The second derivative is necessarily more singular than the first, and hence the dominant balance near a singularity at $\zeta = -\zeta_0$ is

$$-4\zeta_0\frac{\mathrm{d}^2\theta}{\mathrm{d}\zeta^2} \sim -\theta^n. \tag{9}$$

Integrating this equation gives the dominant singular behaviour of $\theta(\zeta)$ as

$$\theta \sim \frac{\gamma_0}{(\zeta+\zeta_0)^\sigma}, \quad \gamma_0 = [4\zeta_0\sigma(\sigma+1)]^{\sigma/2}. \quad \sigma = \frac{2}{n-1}. \tag{10}$$

The singular behaviour (10) differs from that of the singular polytrope [Chandrasekhar p.134, and eq. (19) below] for which $\theta \propto \zeta^{-\sigma/2}$.

The locations of movable singularities depend on the initial condition $\theta(0) = 1$, and must be computed numerically. They are tabulated in Table 1, and shown in Fig. 1. as functions of n, where one sees that the two singularities are equidistant from O at $n = 1.9121$. Appendix A gives a way of computing the values of ζ_0 by numerical integration.

An analysis for the isothermal sphere equation (6) gives its dominant singular behaviour near a movable singularity at $\tilde{\zeta} = -\tilde{\zeta}_0$ as

$$\tilde{\theta} \sim \ln\left[\frac{(\tilde{\zeta}+\tilde{\zeta}_0)^2}{8\tilde{\zeta}_0}\right] - \frac{(\tilde{\zeta}+\tilde{\zeta}_0)}{2\tilde{\zeta}_0} - \frac{(\tilde{\zeta}+\tilde{\zeta}_0)^2}{3\tilde{\zeta}_0^2}\ln(\tilde{\zeta}+\tilde{\zeta}_0) + O(1). \tag{11}$$

Both series analysis and numerical integration show that the isothermal sphere is singular at $\tilde{\zeta} = -\tilde{\zeta}_0 = -10.717029$. This result is not new, having been found by Lampert &

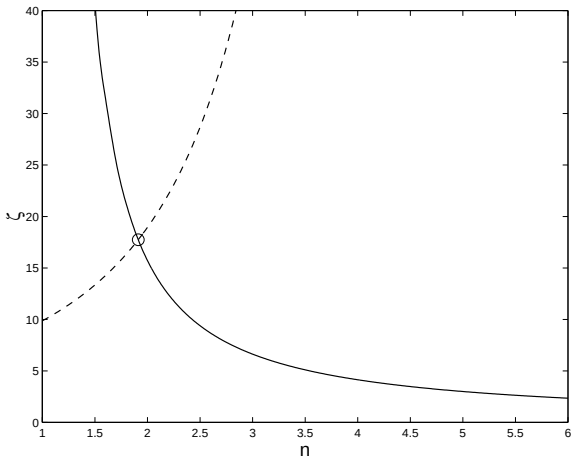

Figure 1. Values of ζ_0 for the singularity (full curve) and ζ_s at the surface (dashed curve) as functions of n, and their crossing at $n = 1.9121$.

Martinelli (1984) in their analysis of a highly charged spherical vesicle, to which the isothermal sphere equation with $\tilde{\zeta} \leq 0$ applies.

Table 1. Coordinates of the singularity and the surface of polytropes.

n	ζ_0	ζ_s
1.00	∞	9.8696
1.25	118.1819	11.4183
1.50	40.9199	13.3499
1.75	23.0939	15.7958
2.00	15.7179	18.9475
2.25	11.7947	23.0930
2.50	9.3915	28.6790
2.75	7.7802	36.4281
3.00	6.6298	47.5665
3.25	5.7696	64.3034
3.50	5.1034	90.9316
3.75	4.5729	136.6630
4.00	4.1408	224.1472
4.25	3.7824	421.4440
4.50	3.4804	1,013.5605
4.75	3.2226	4,407.2468
5.00	3.0000	∞
5.25	2.8059	
5.50	2.6352	
5.75	2.4840	
6.00	2.3491	

Although the positions of the singularities must be determined numerically, one can prove mathematically that they occur at some finite negative value of ζ for any $n > 1$. The proof, which is simple to understand geometrically, uses a phase-plane representation and the (u, v) variables of stellar structure first introduced by Milne (1930). For a polytrope, these variables are

$$u = \frac{-\theta^n}{2(\mathrm{d}\theta/\mathrm{d}\zeta)}, \quad v = \frac{-2\zeta}{\theta}\frac{\mathrm{d}\theta}{\mathrm{d}\zeta}, \tag{12}$$

and they reduce the Lane–Emden equation (3) to the single first order equation

$$\frac{\mathrm{d}v}{\mathrm{d}u} = \frac{v(u+v-1)}{u(3-u-nv)}. \tag{13}$$

Fig. 2 shows the slope field which all solutions must follow. Because $\theta \sim 1 - \zeta/6$ for small ζ, the centre corresponds to the point $u = 3$, $v = 0$ in the phase plane. It is a saddle point through which the solution passes with slope $\mathrm{d}v/\mathrm{d}u = -5/3n$. The physical part of this solution is the segment in the first quadrant. Its continuation to $\zeta < 0$, which is relevant for locating the convergence-limiting movable singularity at $\zeta = \zeta_0$, lies in the fourth quadrant $u > 0$, $v < 0$. The slope field there channels the solution to $u \to \infty$, $v \to -\infty$, and hence to the singularity described by (10). The fact the slope field keeps the solution below the line $u + nv = 3$ is sufficient to prove that the singularity is reached at a finite negative value of ζ whenever $n > 1$. See Appendix A for the detailed argument.

Fig. 3 shows the solution for $\theta(\zeta)$ from negative ζ where it is singular, to the surface of the star at positive ζ. It is plotted for the same $n = 3$ as the phase plane of Fig. 2. Solutions $\theta(\zeta)$ are always concave up, a consequence of equation (A1).

2.3 Series coefficients and singularities

Singularities explain the behaviour of the coefficients a_k of the series (4) for large k. Darboux's theorem (Henrici 1974) states that, when the singular part of $\theta(\zeta)$ at its single closest singularity $\zeta = \zeta_1$ has the form $[1 - \zeta/\zeta_1]^{-\nu} A(\zeta)$, where $A(\zeta)$ is analytic at $\zeta = \zeta_1$, then

$$a_k \sim \frac{A(\zeta_1) k^{\nu-1}}{\Gamma(\nu)\zeta_1^k}\left[1 + O\left(\frac{1}{k}\right)\right], \quad \Gamma(\nu) = (\nu-1)!, \tag{14}$$

$$\frac{a_k}{a_{k+1}} \sim \zeta_1\left[1 + \frac{1-\nu}{k} + O\left(\frac{1}{k^2}\right)\right]. \tag{15}$$

The nonlinearity of the Lane–Emden equation causes the structure of the singularity at $\zeta = -\zeta_0$ to be more complicated than that assumed in Darboux's theorem. It induces other higher order singular terms, such as one in $(1 + \zeta/\zeta_0)^{2+\sigma}$ when 2σ is not an integer, or $(1 + \zeta/\zeta_0)^{2+\sigma} \ln(1 + \zeta/\zeta_0)$ when it is. Consequently these singularities are *always* branch points. Formula (14), which will be used repeatedly in our analysis, is nevertheless valid because of the dominance of the leading $(1 + \zeta/\zeta_0)^{-\sigma}$ term.

The method of Hunter & Guerrieri (1980) makes use of more extensive versions of formula (14) to deduce the locations of singularities and their types without computing the extremely large number of terms needed for the ratios a_k/a_{k+1} to attain their limit. It can deduce the location of the closest singularity of $\theta(\zeta)$ to high accuracy (up to 8 decimal places) for $n \geq 2$ from a relatively modest thirty or forty a_k coefficients, whereas more than 10^8 would be needed for the ratio alone to attain this accuracy.

The fact that the closest singularity occurs at a negative value $\zeta = -\zeta_0$, is the reason for the regular alternation in sign of the coefficients a_k which RS found for $n \geq 2$. The first twenty–one coefficients a_0 through a_{20} of the $n = 1.5$ polytrope alternate in sign, after which later coefficients are all negative. Curiously See (1905) missed that sign change. It can be accounted for by using the approximate formula (14)

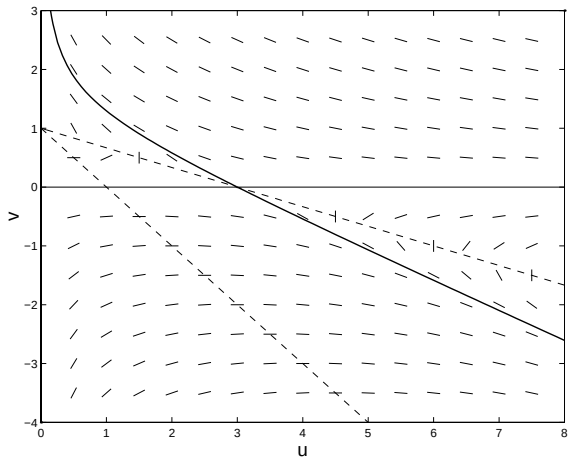

Figure 2. The phase-plane of the Lane–Emden equation for $n = 3$. The thick curve shows the polytrope solution. The short thin lines show slopes defined by equation (13), which are horizontal and vertical respectively at the two dashed lines $u + v = 1$ and $u + nv = 3$.

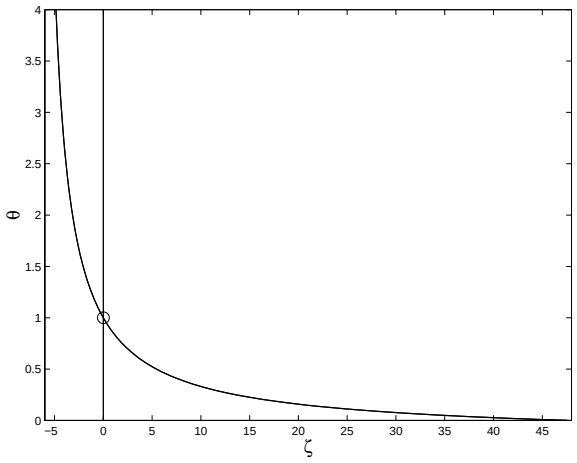

Figure 3. The solution for the $n = 3$ polytrope for both negative and positive ζ.

to evaluate and compare the contributions to a_k from the singularities at $-\zeta_0$ and that at the surface. Formula (14) estimates the ratio of their magnitudes to be $1.99k^{7.5}(\zeta_s/\zeta_0)^k$, using the value $S = -.0278$ for the slope at the surface. The exponential term and the surface singularity eventually dominates, but the large initial factor, due to the near fourth order pole singularity, is so much stronger than the mild $\nu = -3.5$ singularity at the surface, causes this ratio to exceed 2 for $k > 20$.

3 IMPROVING SERIES BY TRANSFORMATION

The physical range for which a series converges can often be extended by a change of the variable in which it is expanded (Van Dyke 1974, Pearce 1978). To be effective, this change must move any convergence-limiting singularity out of the range in which convergence is needed. We consider two transformations that do this in the next two subsections, first the Euler transformation, which is effective for all polytropes *and* for the isothermal sphere, and then the m–series used by RS.

3.1 An Euler transformation

We use an Euler transformation, which, with its inverse, is defined as

$$w = \frac{\zeta}{\zeta + \lambda}, \quad \zeta = \frac{\lambda w}{1 - w}. \tag{16}$$

Here λ is a positive constant which we are free to adjust. The transformation (16) is a one–to–one and everywhere conformal mapping of the *extended* complex ζ–plane, that is the complex ζ–plane plus the point $\zeta = \infty$, to the extended complex w–plane. The physically relevant positive real ζ–axis is compressed to the real interval $0 < w < 1$. The surface of the polytrope at $\zeta = \zeta_s$ maps to $w = w_s = \zeta_s/(\zeta_s + \lambda) < 1$ for $1 \le n < 5$. The fixed singularity at $\zeta = \infty$, which is also the surface for $n \ge 5$, is mapped to $w = 1$. The singularity at $\zeta = -\zeta_0$ is mapped to $w = w_0 = -\zeta_0/(-\zeta_0 + \lambda) < 1$, and so $w_0 > 1$ if $0 < \lambda < \zeta_0$, but $w_0 < -1$ if $\zeta_0 < \lambda < 2\zeta_0$.

3.1.1 Polytropes

To be useful, the Euler transformation must map the singularity at $\zeta = \zeta_0$ further from $w = 0$ than $w = 1$. Convergence of a power series in w is also improved by making w_s as small as possible, and hence as far as possible from the singularity at $w = 1$. To satisfy both requirements, we choose λ as large as possible subject to $\lambda < 2\zeta_0$. This analysis suggests the choice of $\lambda = 13$ for the $n = 3$ polytrope. As confirmation, a 60–term series in w is found to reproduce exactly the seven decimal digits of the whole of Cox & Guili's (1968) Table A.5.2 for this polytrope.

The coefficients of the series expansion

$$\theta = \sum_{k=0}^{\infty} \alpha_k w^k, \quad \theta^n = \sum_{k=0}^{\infty} \beta_k w^k, \quad \alpha_0 = \beta_0 = 1, \tag{17}$$

can in principle all be obtained algebraically from the ζ–series (4) because the centre $\zeta = 0$ maps to $w = 0$. However, I have found this algebraic transformation to be numerically unstable, probably because of the large binomial coefficients which it introduces. I recommend the numerically stable procedure of deriving the w–series directly from the Lane–Emden equation with w as independent variable. That equation is

$$4w(1-w)^3 \frac{\mathrm{d}^2\theta}{\mathrm{d}w^2} + 2(1-w)^2(3-4w)\frac{\mathrm{d}\theta}{\mathrm{d}w} = -\lambda\theta^n \tag{18}$$

Series coefficients are gotten by solving recursively for $k \ge 1$

$$\begin{aligned}\alpha_k =& \frac{1}{2k(2k+1)}[-\lambda\beta_{k-1} + 4(k-1)(3k-1)\alpha_{k-1} \\ & - 2(k-2)(6k-7)\alpha_{k-2} + 4(k-2)(k-3)\alpha_{k-3}],\end{aligned}$$

$$\beta_k = -\frac{1}{k}\sum_{j=0}^{k-1}[n(k-j) - j]\beta_j\alpha_{k-j}. \tag{19}$$

Longer than 60–term series are needed for the outer regions of $n > 3$ polytropes. The fact that, like $\theta(\zeta)$ at $\zeta = \zeta_s$, $\theta(w)$ has a mildly singular $[1 - w/w_s]^{n+2}$ component, when n is not an integer, is not a major problem. Although $w = w_s$ then lies on the circle of convergence, equation (14) predicts that $\alpha_k \sim C/(k^{n+2}w_s^k)$, and the high power of k in the denominator guarantees that the series converges even at the

surface as it does for the $n = 1.5$ polytrope. The major complication is that ζ_s/ζ_0 increases rapidly with increasing n, and so w_s gets close to 1 and approaches the fixed singularity of (18) at $w = 1$. Then equation (14) for a single isolated singularity ceases to be accurate, and convergence becomes much slower in the outer regions. Specifically 120–term and 300–term w–series are needed to obtain $\theta(\zeta)$ to 7–decimal place accuracy all the way out to the surface for $n = 3.5$ and $n = 4$ polytropes respectively.

Polytropes with $n > 5$ have infinite radius, and hence surfaces at the fixed singularity at $\zeta = \infty$. As $\zeta \to \infty$, the solution spirals in to the singular polytrope

$$\theta(\zeta) = [\sigma(1-\sigma)/\zeta]^{\sigma/2}. \tag{20}$$

This means that $\theta(w) \sim [\sigma(1-\sigma)(1-w)/\zeta_0]^{\sigma/2}$ as $w \to 1$, by equation (16). It follows from the approximation (14) that $\alpha_k \propto 1/k^{n/(n-1)}$, and so series (17) for $\theta(w)$ does still converge even at $w = 1$, albeit very slowly.

3.1.2 The Isothermal Sphere

The most interesting $n > 5$ case is that of the isothermal sphere. An Euler transform

$$\tilde{w} = \frac{\tilde{\zeta}}{\tilde{\zeta} + \tilde{\lambda}}, \quad \tilde{\zeta} = \frac{\tilde{\lambda}\tilde{w}}{1 - \tilde{w}}, \tag{21}$$

can be applied to equation (6) and a series expansion

$$\tilde{\theta} = \sum_{k=1}^{\infty} \tilde{\alpha}_k \tilde{w}^k, \quad \tilde{\theta}^n = \sum_{k=0}^{\infty} \tilde{\beta}_k \tilde{w}^k, \quad \tilde{\beta}_0 = 1, \tag{22}$$

derived. The first of the recursion relations for determining the coefficients is the first of equations (19) with tildes added and the sign of the $\tilde{\lambda}$ term changed. The second is the second of equations (8) with a and b replaced by α and β respectively.

The series (22) can not converge at $\tilde{w} = 1$ because $\tilde{\theta}$ becomes infinite as $\tilde{\zeta} \to \infty$ and $\tilde{w} \to 1$. As graphically portrayed in Emden's classic diagram, reproduced as Fig. 19 of Chandrasekhar (1939), the solution spirals in to that of the singular isothermal sphere

$$\tilde{\theta}(\tilde{\zeta}) = \ln\left(\frac{\tilde{\zeta}}{2}\right). \tag{23}$$

Because this singular behavior is known, and is described by $-\ln(1-\tilde{w})$ in terms of $\tilde{w}$, we can separate it out and write

$$\tilde{\theta}(\tilde{w}) = -\ln(1-\tilde{w}) + \sum_{k=1}^{\infty} \left[\tilde{\alpha}_k - \frac{1}{k}\right] \tilde{w}^k. \tag{24}$$

The $1/k$ terms subtracted from the $\tilde{\alpha}_k$ are simply the coefficients of the Taylor series for $\ln(1-\tilde{w})$. The series which remains in equation (24) after the dominant logarithmic singularity (23) has been separated off, is one analytical representation of the decaying spiral. The direct analytical representation is

$$\tilde{\theta}(\tilde{\zeta}) - \ln\left(\frac{\tilde{\zeta}}{2}\right) \sim -\frac{A}{\tilde{\zeta}^{1/4}} \cos\left[\frac{\sqrt{7}}{4}\ln\tilde{\zeta} - \delta\right]. \tag{25}$$

Approximating $\tilde{\zeta}$ as $\tilde{\lambda}/(1-\tilde{w})$ and then applying the approximation (14) to the result, yields

$$\tilde{\alpha}_k - \frac{1}{k} \sim \frac{A}{Gk(\tilde{\lambda}k)^{1/4}} \cos\left[\frac{\sqrt{7}}{4}\ln\left(\tilde{\lambda}k\right) - \delta - \gamma\right]. \tag{26}$$

Here G and γ are constants defined by

$$-\Gamma\left(-\frac{1}{4} + \frac{\mathrm{i}\sqrt{7}}{4}\right) = Ge^{\mathrm{i}\gamma} = 1.1062e^{.6759\mathrm{i}}. \tag{27}$$

This estimate shows that the series (24) converges out to $\tilde{w} = 1$, and hence for the whole of the infinite isothermal sphere. It is only slowly convergent. Though not numerically accurate until very large k, the approximation (26) correctly describes the slow decay with increasing k and the ponderously slow oscillation of the coefficients. With $\tilde{\lambda} = 15$, $\tilde{\alpha}_k - (1/k)$ first changes sign at $k = 39$, and then not again until $k = 5585$. The precise choice of $\tilde{\lambda}$ now matters little, provided that it moves $\tilde{\zeta} = -\tilde{\zeta}_0$ well outside the unit circle and does not exceed $2\tilde{\zeta}_0$.

3.2 Series in the contained mass

Here we summarize the main results from the analysis described in Appendix B. The m–series converges throughout a finite mass $n \le 5$ polytrope because the transformation $\zeta \to m$ maps the singularity at $\zeta = -\zeta_0$ to $m = -\infty$. However, the m–series coefficients u_k decay only as $k^{-(n+2)/(n+1)}$ and so more slowly than the $k^{-(n+2)}$ of the w–series coefficients α_k. The reason for this slow convergence is that the contained mass is not a good variable to use in the outer regions near the surface where the density is so low that contained mass changes very slowly with radius. In fact this causes the function $\theta(m)$ to be a singular function of m when $\theta = 0$. Besides causing the slow convergence for $n < 5$, the singularities at $\theta = 0$ limit the convergence of m–series for polytropes of infinite mass to values of m less than those listed in the second column of Table 2.

4 ANALYTICAL APPROXIMATIONS TO THE ISOTHERMAL SPHERE

The solution $\tilde{\theta}(\tilde{\zeta})$ for the isothermal sphere is singular at $\tilde{\zeta} = -\tilde{\zeta}_0$ as described by equation (11) and as $\tilde{\zeta} \to \infty$ as described by equation (25). Extensive numerical integrations in the complex plane, which were carried out in the course of unravelling the structure described in Appendix B, failed to find any other singularities of $\tilde{\theta}(\tilde{\zeta})$ in $-\pi \le \arg\tilde{\zeta} \le \pi$. We now consider generalisations of the two–term approximations to the isothermal sphere introduced by Natarajan & Lynden-Bell (1997); that is we look for approximations

$$e^{-\tilde{\theta}} \approx \sum_{j=1}^{N} \frac{A_j}{a_j^2 + \tilde{\zeta}}, \tag{28}$$

where the A_j and a_j^2 are constants to be fitted. Natarajan & Lynden-Bell chose this form because its projected density is simple to compute. Their choice is a good one for analytical reasons too. Their simplest approximation of $50/(10+\tilde{\zeta}) - 48/(12+\tilde{\zeta})$ has two simple poles at -10 and -12, with residues of opposite sign and nearly equal magnitudes. Those poles straddle the true singularity at $-\tilde{\zeta}_0 = -10.717$, and approximate that near-double pole [c.f. eq.(11)] well when one is not close to it. The approximation has the correct $2/\tilde{\zeta}$ behaviour at large distances. The accuracy of their optimized approximation, chosen to fit well over the interval $0 \le \tilde{\zeta} \le 100$, is shown in Fig. 4. It deteriorates

at larger distances where it decays as $1.722/\tilde{\zeta}$.

Better accuracy needs more terms, but not many more. Table 2 lists the coefficients of a four-term sum which has relative errors of less than 0.001 per cent in the density throughout $0 \le \tilde{\zeta} \le 1,181$, as is seen in Fig. 4. Those coefficients were chosen to have the correct leading behaviour as $\tilde{\zeta} \to \infty$ by requiring that

$$\sum_{j=1}^{N} A_j = 2. \tag{29}$$

The significance of the range plotted in Fig. 4 is that its upper limit is at a scaled radius of $\tilde{\xi} = 34.363$ where the density is 1/708.61 of its central value. Hence this range is that of an isothermal sphere which is on the brink of gravothermal collapse (Antonov 1962, Lynden-Bell & Wood 1968, Horwitz & Katz 1978).

Table 2. Coefficients for the approximation (28)

j	A_j	a_j^2
1	24.941621	9.229485
2	−22.890004	13.490639
3	−0.602714	106.575159
4	0.551098	5172.242487

The four–term approximation is also dominated by two simple poles which straddle the true singularity at $-\tilde{\zeta}_0$, but it also has two weaker simple poles at much larger negative values of $\tilde{\zeta}$. All but the closest pole lie on the negative $\tilde{\zeta}$ axis to the left of $\tilde{\zeta}_0$, that is they lie on the branch cut needed to make the multivalued function $e^{-\tilde{\theta}}$ single-valued, like the rational approximation (28). It is commonly found that rational approximations to multivalued functions replace branch cuts with alternating zeros and poles (Baker 1975), and the function described by Table 2 in fact has interleaving zeros, one slightly less than a_1^2, another slightly less than a_2^2, and a third at $\tilde{\zeta} = -52.2$. Note that the two weaker singularities also have nearly cancelling residues. This seems to be necessary for accurate approximation, because we had little success with three–term approximations. More than four terms are needed in (28) for accuracy for much larger values of $\tilde{\zeta}$ than 1181, but attempting to use rational approximations out to very large radii is ultimately a pointless exercise, because the isothermal sphere is there described by the spiralling term (25), and is not rational in $\tilde{\zeta}$.

Figure 4 includes also an earlier and more complicated approximation due to Liu (1996). Liu's work was influential in leading Natarajan & Lynden-Bell to finding their simpler model, and to Roxburgh & Stockman (1999) constructing simpler approximations to finite $n < 5$ polytropes. The latter have branch point singularities at negative ζ, which are similar but not identical to those of the true solutions listed in Table 1, just as our four–term approximation does not fit the singularity of the isothermal sphere exactly either. Our finding that these polytrope solutions are dominated by singularities at $-\zeta_0$ and the surface confirms that Roxburgh & Stockman's approach, which approximates both singularities, is well-founded, and that, as they find, one can do better by adding extra terms should better fits for finite polytropes be needed,

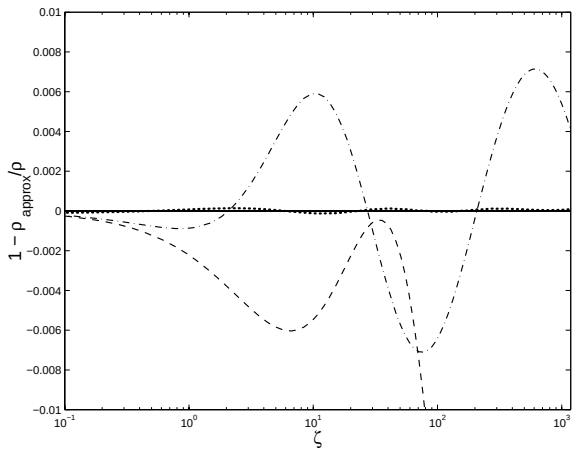

Figure 4. Relative errors in approximating the density of the isothermal sphere for Natarajan & Lynden-Bell's optimized approximation (dashed curve), Liu's approximation (dash–dot line), and equation (28) with the coefficients of Table 2 (dotted line) over the range $0.1 \le \tilde{\zeta} \le 1181$.

5 CONCLUSIONS

We have shown how the Lane-Emden equation for polytropic index $n > 1$ and the isothermal sphere equation develop a prominent singularity at some *negative* value of the squared radius ζ. We have discussed the consequences of that singularity. It limits power series about the centre from converging all the way to the outer surface for $n > 1.9121$. However convergence can be restored by applying an Euler transformation. The singularity at negative ζ is the most significant one for solutions of the Lane-Emden and isothermal sphere equations, and accurate analytical approximations to those solutions need to mimic it well. The approximation to the isothermal sphere derived in Section 4 is an example.

The Euler-transformed series converge significantly faster than the series in the contained mass suggested by Roxburgh & Stockman (1999). The latter do converge all the way to the outer surface $n \le 5$. However they are limited to finite radii for $n > 5$ by a complex conjugate pair of singularities which bifurcate from the finite total mass of the $n = 5$ case. That is a reminder that the convergence of power series is governed by singularities in the complex plane, and hence that one must be wary of what a transformation of variables does to complex as well as real arguments.

ACKNOWLEDGMENTS

Most of this work was done while visiting the Department of Physics, Theoretical Physics, of the University of Oxford, for whose kind hospitality I am grateful. It was also supported in part by the National Science Foundation through grant DMS-9704615.

REFERENCES

Ablowitz M.J., Fokas A.S., 1997, Complex Variables: Introduction and Applications. Cambridge Univ. Press

Antonov, V.A., 1962, Vestnik Leningrad Univ., 7,135 (translated 1985 in Goodman J., Hut P., eds. Dynamics of Star Clusters.

Reidel, Dordrecht, p. 525)
Baker G.A. Jr., 1975, Essentials of Padé Approximants, Chapter 10. Academic Press, New York
Binney J., Tremaine S., 1987, Galactic Dynamics. Princeton Univ. Press, Princeton
Chandrasekhar S., 1939, An Introduction to the Theory of Stellar Structure. Univ. of Chicago Press, Chicago
Cox J.P., Guili R.T., 1968, Principles of Stellar Structure, Chapter 23. Gordon & Breach, London
Emden R., 1907, Gaskugeln. B.G. Teubner, Leipzig
Henrici P., 1974, Applied and Computational Complex Analysis, Chapter 11. John Wiley, New York
Hinch E.J., 1991, Perturbation Methods. Cambridge Univ. Press
Horwitz G., Katz J., 1978, ApJ, 222,941
Hunter C., Guerrieri B., 1980, SIAM J Appl Math, 39, 248
Kippenhahn R., Weigert A., 1990, Stellar Structure and Evolution, Chapter 19. Springer Verlag, Berlin
Lampert M.A., Martinelli R.V., 1984, Chem Phys, 88,399
Liu F.K., 1996, MNRAS, 281,1197
Lynden-Bell D., Wood R., 1968, MNRAS, 138,495
Milne E.A., 1930, MNRAS, 91,4
Natarajan P., Lynden-Bell D., 1997, MNRAS, 286,268
Pearce C.J., 1978, Adv Phys, 27,89
Roxburgh I.R., Stockman L.M., 1999, MNRAS, 303,466 (RS)
See T.J.J., 1905, AN, 169, 322
Van Dyke M.D., 1974, Quart J Mech Appl Math, 27,423

APPENDIX A: PROOF THAT THERE ARE MOVABLE SINGULARITIES AT NEGATIVE ζ

Using the definitions (12) of u and v, the Lane–Emden equation (3) can be written as

$$\frac{\mathrm{d}^2\theta}{\mathrm{d}\zeta^2} = \frac{\theta(-v)(u-3)}{4\zeta^2}. \tag{A1}$$

It follows that $\mathrm{d}^2\theta/\mathrm{d}\zeta^2 > 0$ for $\zeta < 0$ where $v < 0$ and $u > 3$, as well as for $\zeta > 0$ where $v > 0$ and $u < 3$. This guarantees that the graph of θ is concave up, and that $\theta \to \infty$ in $\zeta < 0$, though not necessarily at finite ζ. To show that $\theta \to \infty$ at finite negative ζ, we use the fact that the slope field shown in Fig. 2 forces the solution in $v < 0$ to lie below the line $u + nv = 3$, and hence

$$\frac{u}{(-v)} < n + \frac{3}{(-v)}. \tag{A2}$$

It follows that

$$\frac{u}{(-v)} < n + 1 \quad \text{for} \quad \zeta < -\zeta_*, \tag{A3}$$

where ζ_* denotes the value of ζ at which $v = -3$, and where $\theta = \theta_*$ say. From the definitions of u and v, we have

$$\frac{u}{(-v)} = \frac{\theta^{n+1}}{4(-\zeta)(\mathrm{d}\theta/\mathrm{d}\zeta)^2}. \tag{A4}$$

Substituting this into the inequality(A3), rearranging and integrating gives

$$\int_{\theta_*}^{\theta} \theta'^{-(\frac{n+1}{2})}\mathrm{d}\theta' > \int_{\zeta}^{\zeta_*} \frac{(-\zeta')^{1/2}\mathrm{d}\zeta'}{2\sqrt{n+1}}. \tag{A5}$$

Taking the limit $\theta \to \infty$ for $n > 1$ then gives

$$(-\zeta_*)^{1/2} + \frac{2\sqrt{n+1}}{n-1}\theta_*^{(1-n)/2} > (-\zeta)^{1/2}, \tag{A6}$$

and hence a lower bound on the value of ζ at which $\theta \to \infty$. The proof requires that $n > 1$. That is as it should be it because its result is not true for $n = 1$. The latter is a special case for which the linear Lane-Emden has the exact solution $\theta = \sinh\sqrt{-\zeta}/\sqrt{-\zeta}$ in $\zeta < 0$. It too is concave up for $\zeta < 0$, but does not become infinite until $\zeta \to -\infty$.

The singular value $\zeta = -\zeta_0$ at which $\theta \to \infty$ can be obtained numerically from the ODE

$$\frac{\mathrm{d}u}{\mathrm{d}\zeta} = \frac{u(3-u-nv)}{2\zeta}, \quad \frac{\mathrm{d}v}{\mathrm{d}\zeta} = \frac{v(u+v-1)}{2\zeta}, \tag{A7}$$

by changing to $\ln u$ as independent variable, and then integrating for ζ and $\ln v$ to some large value of $\ln u$, by which stage the asymptotic behaviour (10) is well established.

A similar analysis of the isothermal sphere requires the definitions

$$\tilde{u} = \frac{e^{-\tilde{\theta}}}{2(\mathrm{d}\tilde{\theta}/\mathrm{d}\tilde{\zeta})}, \quad \tilde{v} = 2\tilde{\zeta}\frac{\mathrm{d}\tilde{\theta}}{\mathrm{d}\tilde{\zeta}}, \tag{A8}$$

and gives the phase plane equation

$$\frac{\mathrm{d}\tilde{v}}{\mathrm{d}\tilde{u}} = \frac{\tilde{v}(\tilde{u}-1)}{\tilde{u}(3-\tilde{u}-\tilde{v})}. \tag{A9}$$

The slope field requires that $\tilde{u}+\tilde{v} < 3$ in the fourth quadrant, and hence that $\tilde{u}/(-\tilde{v}) < 2$ for $\tilde{\zeta} < \tilde{\zeta}_*$. Integration now shows that $\tilde{\theta} \to \infty$ for

$$(-\tilde{\zeta}_*)^{1/2} + \frac{1}{2\sqrt{2}}e^{\tilde{\theta}_*/2} > (-\tilde{\zeta})^{1/2}. \tag{A10}$$

APPENDIX B: SERIES IN THE CONTAINED MASS

B1 Finite polytropes

These series, which RS construct, are expansions in the variable m defined by

$$m(\zeta) = q^{2/3} = \zeta\left[-2\frac{\mathrm{d}\theta}{\mathrm{d}\zeta}\right]^{\frac{2}{3}}, \quad q = \int_0^{\xi}\xi'^2\theta^n(\xi')\mathrm{d}\xi'. \tag{B1}$$

Here q is the mass contained within radius ξ, but its power m is the variable in which the power series

$$\theta(m) = \sum_{k=0}^{\infty} u_k m^k, \quad u_0 = 1. \tag{B2}$$

is analytic. RS eq. (11) and (12) give recursive relations for determining the coefficients u_k.

Equation (B1) shows one reason why m–series can converge out to the surface of any $n \le 5$ polytrope; the singularity at $\zeta = -\zeta_0$, at which $\mathrm{d}\theta/\mathrm{d}\zeta$ is infinite, is mapped to $m = -\infty$, and hence much further away than the surface of the polytrope at the finite value $m = m_s = m(\zeta_s)$ which corresponds to its finite mass. RS Fig. 3 for the $n = 1.5$ and $n = 3$ implies that the series (B2) converge slowly for them. The rate at which they converge can also be deduced from (14). It is governed by the form of the singularity of $\theta(m)$ at $m = m_s$, where $\mathrm{d}m/\mathrm{d}\zeta$ vanishes because it is proportional to θ^n, and hence to $(\zeta_s - \zeta)^n$. It follows that $\theta \propto (\zeta_s - \zeta) \propto (m_s - m)^{1/(n+1)}$, and, unlike $\theta(\zeta)$, is singular at the surface even for integer n. The value $\nu = -1/(n+1)$ is needed in the estimate (14), which then predicts $u_k \propto 1/m_s^k k^{(n+2)/(n+1)}$. The closeness of the power of k to 1 explains why the m–series converge so slowly near

the surface, much more slowly than the corresponding Euler-transformed series. The series coefficients u_k are all negative for $k \geq 1$, as RS find, because the surface value $m = m_s$ is then the singularity closest to $m = 0$.

B2 Infinite polytropes and the Isothermal Sphere

The $n = 5$ polytrope, for which an exact integral of the Lane-Emden equation is known, lies on the boundary between finite polytropes of finite radius and finite mass, and infinite polytropes of infinite radius and infinite mass. It has infinite radius but finite mass. It is described analytically by

$$\theta = \frac{1}{(1+\zeta/3)^{1/2}} = \left[1 - \frac{m}{3^{1/3}}\right]^{1/2}. \tag{B3}$$

The coefficients u_k of its m–series are negative for all $k \geq 1$, but a different behaviour sets in for $n > 5$. Then the u_k alternate in sign between equal, or nearly equal, blocks. In the case of the isothermal sphere, most of these blocks are of length 4, but interspersed with occasional blocks of length 5. The average length of blocks of the same sign is 4.18. Such behaviour indicates a conjugate pair of singularities. When there is such a pair at $m = m_1 e^{\pm i\mu}$, near which

$$\theta(m) \sim C e^{i\gamma} \left[1 - \frac{m}{m_1 e^{\pm i\mu}}\right]^{-\nu}, \tag{B4}$$

formula (14) predicts that the asymptotic form of the coefficients for large k is

$$u_k \sim \frac{2Ck^{\nu-1}}{m_1^k \Gamma(\nu)} \cos(k\mu - \gamma). \tag{B5}$$

The cosine factor predicts regular changes of sign whenever k increases by π/μ. A sign change for every increase of 4.18 in k therefore indicates a pair of singularities at angles of $\pm\mu = \pm.7516 = \pm 43.06°$, Formula (B5) allows us to estimate that $m_1 = 11.43$, and hence that the m-series for the isothermal sphere converges only for $|\tilde{\xi}| < 16.4$.

The u_k coefficients for $n > 5$ polytropes can be analyzed in the same way. They too show convergence-limiting singularities complex singularities at the values listed in Table 3. Plotting their locations in the complex m–plane suggests strongly, and correctly, that these complex singularities are linked to the zeros of $\theta(m)$ at finite real values of m for polytropes with $n \leq 5$. The last of these is that of the $n = 5$ polytrope at $m = 3^{1/3}$, after which the polytropes are suddenly infinitely massive, and there can be no more real zeros of $\theta(m)$. The zeros of $\theta(m)$ do not disappear though; they split in two and move off the real axis to form a conjugate pair. Complex singularities must occur in conjugate pairs because $\theta(m)$ is real for real m.

Table 3. Properties of the complex singularities in m

n	m_1	μ_{crit}	$\lvert\zeta\rvert$	$\pm\arg\zeta$
2	1.798	0.		
3	1.597	0.		
4	1.478	0.		
5	1.442	0.		
6	1.437	0.103	421.785	6.820
7	1.337	0.200	95.512	7.228
8	1.227	0.274	36.228	7.487
10	1.034	0.375	9.610	7.789
12	0.885	0.442	3.806	7.958
15	0.724	0.506	1.381	8.104
20	0.553	0.570	0.425	8.232

To confirm that the complex singularities occur at zeros of $\theta(m)$, and to find where these zeros lie in the ζ–plane, we recast the Lane-Emden equation as a pair of first order equations for θ and ζ as functions of m:

$$\frac{\mathrm{d}\theta}{\mathrm{d}m} = \frac{-3m^2}{2\zeta^2\theta^n}, \quad \frac{\mathrm{d}\zeta}{\mathrm{d}m} = \frac{3}{\theta^n}\left(\frac{m}{\zeta}\right)^{1/2}. \tag{B6}$$

Then we integrate out from $m = 0$ (the centre of the sphere) along rays $m = Me^{i\mu}$ with M increasing and μ constant, and track the images of these rays in the complex ζ–plane. For $\mu = 0$ and for a class of adjacent and sufficiently small μ values, $|\zeta| \to \infty$ in the direction $\arg\zeta = [3(n-1)\mu]/(n-3)$. This is because the solution tends to the singular solution (20), and $\theta \propto m^{3/(3-n)}$ asymptotically. For $\mu = \pi$ and for an adjacent class of lesser μ values, ζ trends to $-\zeta_0$ as $M \to \infty$. By equations (10) and (B1), this approach is along a ray making an angle $[3(n-1)(\pi-\mu)]/2(n+1)$ with the real ζ–axis. The transition between these two classes occurs at some value $\mu = \mu_{crit}$, and is abrupt. Integrations along the rays of constant μ allow one to determine the value of μ_{crit} accurately, but do not give accurate solutions for θ and ζ for the regions in which $|\theta|$ is small. That is because, as equations (B6) show, small changes in m cause large changes in θ and ζ. To avoid this problem, we first discover where to look in the ζ–plane, and then integrate the Lane-Emden equation (3) with ζ as independent variable, locate the zero of θ, and calculate its value of m. That value is $m_1 e^{i\mu_{crit}}$. Values found in this way are close to the estimates obtained from analysis of m–series.

Table 3 lists also where the convergence-limiting zeros of $\theta(m)$ lie in the complex ζ–plane. These points, which move in from $\zeta = \infty$ as n increases from 5, all have angular arguments larger in magnitude than 2π. They all lie on sheets of the Riemann surface of $\theta(\zeta)$ which are reached after encircling its branch point at $\zeta = -\zeta_0$. The mapping $\zeta \to m$, which is a simple one-to-one bilinear mapping $m = 3^{1/3}\zeta/(\zeta+3)$ for $n = 5$ becomes more complicated for $n > 5$.

The corresponding analysis for the isothermal sphere uses the equations

$$\frac{\mathrm{d}\tilde{\theta}}{\mathrm{d}\tilde{m}} = \frac{3\tilde{m}^2}{2\tilde{\zeta}^2} e^{\tilde{\theta}}, \quad \frac{\mathrm{d}\tilde{\zeta}}{\mathrm{d}\tilde{m}} = 3\left(\frac{\tilde{m}}{\tilde{\zeta}}\right)^{1/2} e^{\tilde{\theta}}, \tag{B7}$$

where now,

$$\tilde{m}(\tilde{\zeta}) = \tilde{q}^{2/3} = \tilde{\zeta}\left[2\frac{\mathrm{d}\tilde{\theta}}{\mathrm{d}\tilde{\zeta}}\right]^{\frac{2}{3}}, \quad \tilde{q} = \int_0^{\tilde{\xi}} \tilde{\xi}'^2 e^{-\tilde{\theta}}(\tilde{\xi}')\mathrm{d}\tilde{\xi}'. \tag{B8}$$

It is different in only one essential respect. The critical ray

which separates the rays with $0 \le \mu < \mu_{crit}$ which go to $\tilde{\zeta} = \infty$ from those with $\mu_{crit} < \mu \le \pi$ which tend to $\tilde{\zeta} = -\tilde{\zeta}_0$, now goes to a zero of $e^{-\tilde{\theta}}$ rather than to one of θ. That is it goes to a singularity at which $\Re(\tilde{\theta}) \to \infty$. Equation (6) permits such a singularity to occur only when $\tilde{\zeta} = 0$. There is no singularity at the centre of the sphere where we require the solution to be analytic. Rather the singularities occur at the two $\tilde{\zeta} = 0$ points reached after encircling the logarithmic branch point at $\tilde{\zeta} = -\tilde{\zeta}_0$ once in either direction. The local density $e^{-\tilde{\theta}}$ is negligible near either point, and so the isothermal sphere equation reduces locally to Laplace's equation, and its solution is the point mass potential

$$\tilde{\theta} \sim 8.0451 \pm 2.6875\mathrm{i} + \frac{C}{\tilde{\zeta}^{1/2}}, \quad C = -16.6773 \mp 34.9315\mathrm{i}. \tag{B9}$$

The corresponding value of $\tilde{m}$ are $\lim_{\tilde{\zeta}\to 0}[\tilde{\zeta}(-C\tilde{\zeta}^{-3/2})^{2/3}] = 11.4429e^{\pm .75025\mathrm{i}}$. These two complex point masses on Riemann surface extensions of physical space are what limits the usefulness of the real $\tilde{m}$–series for the isothermal sphere!

APPENDIX C: THE ISOTHERMAL SPHERE AS THE $N \to \infty$ LIMIT OF A POLYTROPE

The isothermal sphere equation (6) is not obtained by letting $n \to \infty$ in the Lane-Emden equation (3). Instead one must first choose a new scaled polytrope potential which vanishes at the centre and increases outwards like that of the isothermal sphere. We define a new potential $\tilde{\theta}$ and a new scaled independent variable $\tilde{\zeta}$ for polytropes via the relations

$$\tilde{\theta} = n(1-\theta), \quad \tilde{\zeta} = n\zeta. \tag{C1}$$

Then the Lane-Emden equation (3) becomes

$$4\tilde{\zeta}\frac{\mathrm{d}^2\tilde{\theta}}{\mathrm{d}\tilde{\zeta}^2} + 6\frac{\mathrm{d}\tilde{\theta}}{\mathrm{d}\tilde{\zeta}} = \left[1 - \frac{\tilde{\theta}}{n}\right]^n. \tag{C2}$$

Now we can take the $n \to \infty$ limit. The right hand side becomes $e^{-\tilde{\theta}}$, and we recover the isothermal equation (6).

The form of this transformation explains several otherwise puzzling features of this study. The n in the rescaling (C1) of the independent variable explains why its $\tilde{\zeta}_0$ exceeds most of the ζ_0 values in Table 1, which are much smaller and are evidently decreasing with increasing n. It is this sequence multiplied by n which tends to $\tilde{\zeta}_0$. Likewise

$$m(\zeta) = q^{2/3} = \zeta\left[-2\frac{\mathrm{d}\theta}{\mathrm{d}\zeta}\right]^{\frac{2}{3}} \to \frac{\tilde{\zeta}}{n}\left[2\frac{\mathrm{d}\tilde{\theta}}{\mathrm{d}\tilde{\zeta}}\right]^{\frac{2}{3}} = \frac{\tilde{m}}{n}, \tag{C3}$$

and the value $\tilde{m} = 11.443$ is the limit of n times the m values in Table 3, while $n|\zeta|$ tends to zero because the singularities tend to $\tilde{\zeta} = 0$.

When the new variables (C1) are introduced into the definitions (12) of u and v and the $n \to \infty$ limit taken, we obtain new variables $\tilde{u}$ and $\tilde{v}$ and as follows:

$$u = \frac{-\theta^n}{2(\mathrm{d}\theta/\mathrm{d}\zeta)} \to \frac{e^{-\tilde{\theta}}}{2(\mathrm{d}\tilde{\theta}/\mathrm{d}\tilde{\zeta})} = \tilde{u},$$

$$v = \frac{-2\zeta}{\theta}\frac{\mathrm{d}\theta}{\mathrm{d}\zeta} \to 2\tilde{\zeta}\frac{\mathrm{d}\tilde{\theta}}{n\mathrm{d}\tilde{\zeta}} = \frac{\tilde{v}}{n}. \tag{C4}$$

The presence of n in the relation between the v and $\tilde{v}$ is why equation (A9) is the $n \to \infty$ limit of equation (13).

The transformation (C1) allows the series solution for the isothermal sphere to be derived from that for polytropes via the relation

$$\tilde{a}_k = \lim_{n\to\infty} -n^{1-k}a_k, \qquad k \ge 1.$$

This paper has been produced using the Royal Astronomical Society/Blackwell Science TEX macros.